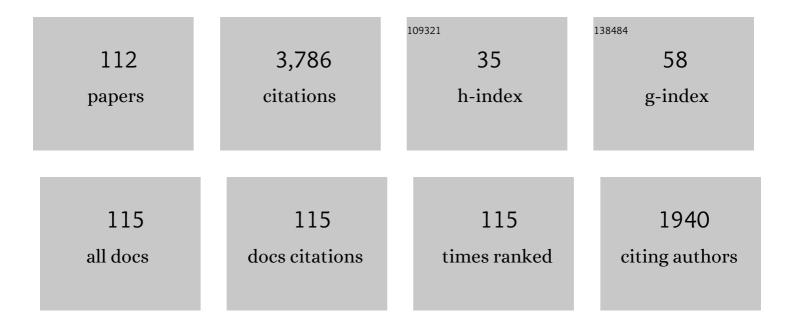
Antonio Rius

List of Publications by Year in descending order

Source: https://exaly.com/author-pdf/5242251/publications.pdf Version: 2024-02-01



Δητόμιο Ριμε

#	Article	IF	CITATIONS
1	Standard Deviation of Spaceborne GNSS-R Ocean Scatterometry Measurements. IEEE Transactions on Geoscience and Remote Sensing, 2022, 60, 1-16.	6.3	Ο
2	Exploration of Multi-Mission Spaceborne GNSS-R Raw IF Data Sets: Processing, Data Products and Potential Applications. Remote Sensing, 2022, 14, 1344.	4.0	19
3	First spaceborne demonstration of BeiDou-3 signals for GNSS reflectometry from CYGNSS constellation. Chinese Journal of Aeronautics, 2021, 34, 1-10.	5.3	23
4	Assessment of Spaceborne GNSS-R Ocean Altimetry Performance Using CYGNSS Mission Raw Data. IEEE Transactions on Geoscience and Remote Sensing, 2020, 58, 238-250.	6.3	78
5	Variational Retrievals of High Winds Using Uncalibrated CyGNSS Observables. Remote Sensing, 2020, 12, 3930.	4.0	15
6	First Precise Spaceborne Sea Surface Altimetry With GNSS Reflected Signals. IEEE Journal of Selected Topics in Applied Earth Observations and Remote Sensing, 2020, 13, 102-112.	4.9	64
7	Measuring Greenland Ice Sheet Melt Using Spaceborne GNSS Reflectometry From TechDemoSatâ€1. Geophysical Research Letters, 2020, 47, e2019GL086477.	4.0	15
8	Experimental Validation of GNSS Interferometric Radio Occultation. Remote Sensing, 2019, 11, 2758.	4.0	1
9	Applications of Spaceborne GNSS-R over Inland Waters and Wetlands. , 2019, , .		6
10	ls Accurate Synoptic Altimetry Achievable by Means of Interferometric GNSS-R?. Remote Sensing, 2019, 11, 505.	4.0	11
11	Sensing Heavy Precipitation With GNSS Polarimetric Radio Occultations. Geophysical Research Letters, 2019, 46, 1024-1031.	4.0	26
12	Effects of PRN-Dependent ACF Deviations on GNSS-R Wind Speed Retrieval. IEEE Geoscience and Remote Sensing Letters, 2019, 16, 327-331.	3.1	17
13	Revisiting the GNSS-R Waveform Statistics and Its Impact on Altimetric Retrievals. IEEE Transactions on Geoscience and Remote Sensing, 2018, 56, 2854-2871.	6.3	65
14	GNSS Transpolar Earth Reflectometry exploriNg System (G-TERN): Mission Concept. IEEE Access, 2018, 6, 13980-14018.	4.2	55
15	Bi-Static Reflectometry Using Soop for Atmospheric Applications. , 2018, , .		Ο
16	Polarimetric Gnss Radio-Occultations Aboard Paz: Commissioning Phase and Preliminary Results. , 2018, , .		1
17	Lake Level and Surface Topography Measured With Spaceborne GNSSâ€Reflectometry From CYGNSS Mission: Example for the Lake Qinghai. Geophysical Research Letters, 2018, 45, 13,332.	4.0	71
18	Detection and Measurement of Moving Targets Using X-band Digital Satellite TV Signals. , 2018, , .		2

#	Article	IF	CITATIONS
19	Reflectometry. , 2017, , 1163-1186.		3
20	First spaceborne phase altimetry over sea ice using TechDemoSatâ€1 GNSSâ€R signals. Geophysical Research Letters, 2017, 44, 8369-8376.	4.0	150
21	Electron density extrapolation above F2 peak by the linear Varyâ€Chap model supporting new Global Navigation Satellite Systemsâ€LEO occultation missions. Journal of Geophysical Research: Space Physics, 2017, 122, 9003-9014.	2.4	30
22	Advances in GNSS-R altimetry. , 2017, , .		1
23	WAVPY: A GNSS-R open source software library for data analysis and simulation. , 2017, , .		26
24	A Software-Defined GNSS Reflectometry Recording Receiver with Wide-Bandwidth, Multi-Band Capability and Digital Beam-Forming. Remote Sensing, 2017, 9, 450.	4.0	18
25	Feasibility of GNSS-R Ice Sheet Altimetry in Greenland Using TDS-1. Remote Sensing, 2017, 9, 742.	4.0	36
26	Prediction of GNSS-R altimetry precision based on waveform statistics. , 2017, , .		0
27	Untangling rain structure from polarimetric GNSS Radio Occultation observables: a 2D tomographic approach. European Journal of Remote Sensing, 2016, 49, 571-585.	3.5	5
28	The Impact of Inter-Modulation Components on Interferometric GNSS-Reflectometry. Remote Sensing, 2016, 8, 1013.	4.0	11
29	GEROS-ISS: GNSS REflectometry, Radio Occultation, and Scatterometry Onboard the International Space Station. IEEE Journal of Selected Topics in Applied Earth Observations and Remote Sensing, 2016, 9, 4552-4581.	4.9	99
30	Atmospheric polarimetric effects on GNSS radio occultations: the ROHP-PAZ field campaign. Atmospheric Chemistry and Physics, 2016, 16, 635-649.	4.9	30
31	Initial Results of Typhoon Wind Speed Observation Using Coastal GNSS-R of BeiDou GEO Satellite. IEEE Journal of Selected Topics in Applied Earth Observations and Remote Sensing, 2016, 9, 4720-4729.	4.9	31
32	Mitigation of Direct Signal Cross-Talk and Study of the Coherent Component in GNSS-R. IEEE Geoscience and Remote Sensing Letters, 2015, 12, 279-283.	3.1	32
33	Sensitivity of PAZ LEO Polarimetric GNSS Radio-Occultation Experiment to Precipitation Events. IEEE Transactions on Geoscience and Remote Sensing, 2015, 53, 190-206.	6.3	38
34	Consolidating the Precision of Interferometric GNSS-R Ocean Altimetry Using Airborne Experimental Data. IEEE Transactions on Geoscience and Remote Sensing, 2014, 52, 4992-5004.	6.3	130
35	Experimental Evaluation of GNSS-Reflectometry Altimetric Precision Using the P(Y) and C/A Signals. IEEE Journal of Selected Topics in Applied Earth Observations and Remote Sensing, 2014, 7, 1493-1500.	4.9	33
36	Optimization and Performance Analysis of Interferometric GNSS-R Altimeters: Application to the PARIS IoD Mission. IEEE Journal of Selected Topics in Applied Earth Observations and Remote Sensing, 2014, 7, 1436-1451.	4.9	58

#	Article	IF	CITATIONS
37	Experimental Results of an X-Band PARIS Receiver Using Digital Satellite TV Opportunity Signals Scattered on the Sea Surface. IEEE Transactions on Geoscience and Remote Sensing, 2014, 52, 5704-5711.	6.3	31
38	Delay Tracking in Spaceborne GNSS-R Ocean Altimetry. IEEE Geoscience and Remote Sensing Letters, 2013, 10, 57-61.	3.1	26
39	GNSS-R Derived Centimetric Sea Topography: An Airborne Experiment Demonstration. IEEE Journal of Selected Topics in Applied Earth Observations and Remote Sensing, 2013, 6, 1468-1478.	4.9	37
40	PARIS Interferometric Technique proof of concept: Sea surface altimetry measurements. , 2012, , .		22
41	Submeter ocean altimetry with GPS L1 C/A signal. , 2012, , .		2
42	Interferometric GNSS-R achievable altimetric performance and compression/denoising using the wavelet transform: An experimental study. , 2012, , .		8
43	Phase Altimetry With Dual Polarization GNSS-R Over Sea Ice. IEEE Transactions on Geoscience and Remote Sensing, 2012, 50, 2112-2121.	6.3	91
44	Pycaro's instrument proof of concept. , 2012, , .		5
45	Characterization of dry-snow sub-structure using GNSS reflected signals. Remote Sensing of Environment, 2012, 124, 122-134.	11.0	73
46	On the retrieval of the specular reflection in GNSS carrier observations for ocean altimetry. Radio Science, 2012, 47, .	1.6	25
47	Review of the CALIMAS Team Contributions to European Space Agency's Soil Moisture and Ocean Salinity Mission Calibration and Validation. Remote Sensing, 2012, 4, 1272-1309.	4.0	11
48	Altimetry with GNSS-R interferometry: first proof of concept experiment. GPS Solutions, 2012, 16, 231-241.	4.3	81
49	Detection of Arctic Ocean tides using interferometric GNSS-R signals. Geophysical Research Letters, 2011, 38, n/a-n/a.	4.0	60
50	GNSSâ€R groundâ€based and airborne campaigns for ocean, land, ice, and snow techniques: Application to the GOLDâ€RTR data sets. Radio Science, 2011, 46, .	1.6	108
51	Heterogeneous transmission and parallel computing platform (HTPCP) for remote sensing applications. Proceedings of SPIE, 2011, , .	0.8	0
52	Preliminary error budget of a GNSS-R spaceborne mission. , 2011, , .		1
53	One-bit digital cross-correlation in the PARIS-IOD. , 2011, , .		1
54	CAROLS: A New Airborne L-Band Radiometer for Ocean Surface and Land Observations. Sensors, 2011, 11, 719-742.	3.8	51

#	Article	IF	CITATIONS
55	Monitoring sea-ice and dry snow with GNSS reflections. , 2010, , .		24
56	Altimetric Analysis of the Sea-Surface GPS-Reflected Signals. IEEE Transactions on Geoscience and Remote Sensing, 2010, 48, 2119-2127.	6.3	140
57	GNSS Signal Interference Classified by Means of a Supervised Learning Method Applied in the Time-Frequency Domain. , 2009, , .		3
58	Parallel workload analysis in SMP platform: a new modelling approach to infer the hardware efficiency for remote sensing application. Proceedings of SPIE, 2009, , .	0.8	1
59	A new technique to sense non-Gaussian features of the sea surface from L-band bi-static GNSS reflections. Remote Sensing of Environment, 2008, 112, 2927-2937.	11.0	52
60	Sea surface slopes' PDF from GNSS reflected signals. , 2007, , .		3
61	ASAP, towards a PARIS instrument for space. , 2007, , .		0
62	A GPS-Reflections Receiver That Computes Doppler/Delay Maps in Real Time. IEEE Transactions on Geoscience and Remote Sensing, 2007, 45, 156-174.	6.3	81
63	Panic anxiety, under the weather?. International Journal of Biometeorology, 2005, 49, 238-243.	3.0	35
64	SCALES: SEVIRI and GERB CaL/VaL area for large-scale field experiments. , 2004, , .		1
65	A raytracing inversion procedure for the extraction of the atmospheric refractivity from GNSS travel-time data. Physics and Chemistry of the Earth, 2004, 29, 213-224.	2.9	8
66	Three-Dimensional Variational Data Assimilation of Ground-Based GPS ZTD and Meteorological Observations during the 14 December 2001 Storm Event over the Western Mediterranean Sea. Monthly Weather Review, 2004, 132, 749-763.	1.4	57
67	Mediterranean Balloon Experiment: ocean wind speed sensing from the stratosphere, using GPS reflections. Remote Sensing of Environment, 2003, 88, 351-362.	11.0	80
68	Sea surface state measured using GPS reflected signals. Geophysical Research Letters, 2002, 29, 37-1-37-4.	4.0	92
69	MM5 derived ZWDs compared to observational results from VLBI, GPS and WVR. Physics and Chemistry of the Earth, 2002, 27, 301-308.	2.9	14
70	Integrating NWP products into the analysis of GPS observables. Physics and Chemistry of the Earth, 2002, 27, 377-383.	2.9	6
71	Zenith total delay study of a mesoscale convective system: GPS observations and fine-scale modeling. Tellus, Series A: Dynamic Meteorology and Oceanography, 2002, 54, 138-147.	1.7	7
72	Tomography of the lower troposphere using a small dense network of GPS receivers. IEEE Transactions on Geoscience and Remote Sensing, 2001, 39, 439-447.	6.3	44

#	Article	IF	CITATIONS
73	lonospheric tomography using Ã~rsted GPS measurements - preliminary results. Physics and Chemistry of the Earth, 2001, 26, 173-176.	0.6	9
74	Spatio-temporal tomography of the lower troposphere using GPS signals. Physics and Chemistry of the Earth, 2001, 26, 405-411.	0.6	7
75	Comparison of software and techniques for water vapor estimation using German near real-time GPS data. Physics and Chemistry of the Earth, 2001, 26, 417-420.	0.6	2
76	The contributions of the MAGIC project to the COST 716 objectives of assessing the operational potential of ground-based GPS meteorology on an international scale. Physics and Chemistry of the Earth, 2001, 26, 433-437.	0.6	19
77	The Use of GPS to Validate NWP Systems: The HIRLAM Model. Journal of Atmospheric and Oceanic Technology, 2000, 17, 773-787.	1.3	39
78	A near real time system for tropospheric monitoring using IGS hourly data. Earth, Planets and Space, 2000, 52, 681-684.	2.5	5
79	Sensing atmospheric structure: Tropospheric tomographic results of the small-scale GPS campaign at the Onsala Space Observatory. Earth, Planets and Space, 2000, 52, 941-945.	2.5	12
80	The use of GPS buoys in the determination of oceanic variables. Earth, Planets and Space, 2000, 52, 1113-1116.	2.5	12
81	A PIM-aided kalman filter for gps tomography of the ionospheric electron content. Physics and Chemistry of the Earth, Part C: Solar, Terrestrial and Planetary Science, 1999, 24, 365-369.	0.2	6
82	Estimation of tropospheric zenith delay and gradients over the Madrid area using GPS and WVR data. Geophysical Research Letters, 1999, 26, 447-450.	4.0	27
83	Sensing atmospheric structure using small-scale space geodetic networks. Geophysical Research Letters, 1999, 26, 2445-2448.	4.0	32
84	Deep 8.4 GHz VLBI Images of Seven Faint Nuclei in Lobeâ€dominated Quasars. Astrophysical Journal, 1999, 511, 84-104.	4.5	10
85	Spanish Participation in the Millimeter Array. Astrophysics and Space Science, 1998, 263, 381-388.	1.4	Ο
86	GPS tomography of the ionospheric electron content with a correlation functional. IEEE Transactions on Geoscience and Remote Sensing, 1998, 36, 143-153.	6.3	51
87	Analysis of ionospheric electron density distribution from GPS/MET occultations. IEEE Transactions on Geoscience and Remote Sensing, 1998, 36, 383-394.	6.3	43
88	lonospheric calibration of radar altimeters using GPS tomography. Geophysical Research Letters, 1998, 25, 3771-3774.	4.0	13
89	Incorporation of GPS data into a parameterized ionospheric model for tomography of the electron distribution of the ionosphere. , 1998, 3495, 397.		1
90	VLBI Observations of Supernova 1993J: The First 1000 Days. International Astronomical Union Colloquium, 1998, 164, 355-356.	0.1	0

#	Article	IF	CITATIONS
91	Use of global navigation satellite systems for the atmospheric calibration of radar altimeters. , 1998, ,		0
92	A two-layer model of the ionosphere using Global Positioning System data. Geophysical Research Letters, 1997, 24, 393-396.	4.0	69
93	Improving the vertical resolution of ionospheric tomography with GPS Occultations. Geophysical Research Letters, 1997, 24, 2291-2294.	4.0	94
94	VLBI Observations of the Ultracompact Radio Nucleus of the Galaxy M81. Astrophysical Journal, 1996, 457, 604.	4.5	43
95	Measuring geocentric radial coordinates with a non-fiducial GPS network. Bulletin Geodesique, 1995, 69, 320-328.	0.4	4
96	Discovery of shell-like radio-structure in SN1993J. Nature, 1995, 373, 44-45.	27.8	47
97	Expansion of SN 1993J. Science, 1995, 270, 1475-1478.	12.6	48
98	Proper Motion of Components in 4C 39.25. Astronomical Journal, 1995, 110, 2586.	4.7	24
99	Ionospheric calibration of single frequency VLBI and GPS observations using dual GPS data. Bulletin Geodesique, 1994, 68, 230-235.	0.4	6
100	The shape, expansion rate and distance of supernova 1993J from VLBI measurements. Nature, 1994, 368, 610-613.	27.8	44
101	Relative motions in Europe studied with a geodetic VLBI network. Geophysical Journal International, 1994, 117, 763-768.	2.4	13
102	Estimation of the transmitter and receiver differential biases and the ionospheric total electron content from Global Positioning System observations. Radio Science, 1994, 29, 577-586.	1.6	384
103	Radio-size estimates of SN 1993J. Astrophysical Journal, 1994, 424, L25.	4.5	19
104	Centimeter repeatability of the VLBI estimates of European baselines. Bulletin Geodesique, 1992, 66, 21-26.	0.4	6
105	A high-resolution radio image of a young supernova. Nature, 1991, 350, 212-214.	27.8	33
106	Radio light curve of the periodic radio star LSI+61�303 AT 3.6 CM wavelength. Astrophysics and Space Science, 1990, 169, 203-204.	1.4	1
107	A search at the millijansky level for milli-arcsecond cores in a complete sample of radio galaxies. Astrophysical Journal, 1984, 284, 519.	4.5	1
108	VLBI observations of the polarized radio emission from the quasar 3C 454.3. Astrophysical Journal, 1984, 286, 503.	4.5	27

#	Article	IF	CITATIONS
109	The milli-arcsecond images of Q0957 + 561. Astrophysical Journal, 1984, 287, 538.	4.5	30
110	Detection of a Compact Radio Source near the Center of a Gravitational Lens: Quasar Image or Galactic Core?. Science, 1983, 219, 54-56.	12.6	27
111	The very flat radio spectrum of 0735 plus 178 - A cosmic conspiracy. Astrophysical Journal, 1980, 238, L123.	4.5	64
112	A 3 GPS-channels Doppler-delay receiver for remote sensing applications. , 0, , .		6